Cerebral Cortex May 2012;22:1016-1024
doi:10.1093/cercor/bhr176
Advance Access publication July 19, 2011

The Effect of Preterm Birth on Thalamic and Cortical Development

Gareth Ball[1], James P. Boardman[1,2], Daniel Rueckert[3], Paul Aljabar[3], Tomoki Arichi[1,4], Nazakat Merchant[1,4], Ioannis S. Gousias[1], A. David Edwards[1,4] and Serena J. Counsell[1]

[1]Centre for the Developing Brain, Imperial College London and MRC Clinical Sciences Centre, Hammersmith Hospital, London W12 0NN, UK, [2]Simpson Centre for Reproductive Health, Royal Infirmary of Edinburgh, Edinburgh EH16 4SA, UK, [3]Biomedical Image Analysis Group, Department of Computing, Imperial College London, London SW7 2AZ, UK and [4]Division of Neonatology, Imperial College Healthcare NHS Trust, London W12 0HS, UK

Address correspondence to Serena J. Counsell, Robert Steiner MR Unit, Imaging Sciences Department, Imperial College London, Hammersmith Hospital, DuCane Road, London W12 0HS, UK. Email: serena.counsell@imperial.ac.uk.

Preterm birth is a leading cause of cognitive impairment in childhood and is associated with cerebral gray and white matter abnormalities. Using multimodal image analysis, we tested the hypothesis that altered thalamic development is an important component of preterm brain injury and is associated with other macro- and microstructural alterations. T_1- and T_2-weighted magnetic resonance images and 15-direction diffusion tensor images were acquired from 71 preterm infants at term-equivalent age. Deformation-based morphometry, Tract-Based Spatial Statistics, and tissue segmentation were combined for a nonsubjective whole-brain survey of the effect of prematurity on regional tissue volume and microstructure. Increasing prematurity was related to volume reduction in the thalamus, hippocampus, orbitofrontal lobe, posterior cingulate cortex, and centrum semiovale. After controlling for prematurity, reduced thalamic volume predicted: lower cortical volume; decreased volume in frontal and temporal lobes, including hippocampus, and to a lesser extent, parietal and occipital lobes; and reduced fractional anisotropy in the corticospinal tracts and corpus callosum. In the thalamus, reduced volume was associated with increased diffusivity. This demonstrates a significant effect of prematurity on thalamic development that is related to abnormalities in allied brain structures. This suggests that preterm delivery disrupts specific aspects of cerebral development, such as the thalamocortical system.

Keywords: brain development, deformation-based morphometry, DTI, cortex, TBSS, thalamus

Introduction

Preterm birth is rapidly emerging as a leading cause of neurodevelopmental impairment in childhood. With advances in neonatal intensive care, mortality has decreased considerably but there is a high prevalence of cognitive and behavioral deficits in up to 50% of surviving preterm infants in childhood (Marlow et al. 2005; Delobel-Ayoub et al. 2009). Understanding the neural substrates for impairment in this population is essential for designing mechanistic and therapeutic studies and may provide further insight into the development of systems that underlie human cognition.

Evidence from in vivo magnetic resonance imaging (MRI) studies has identified a number of cerebral abnormalities in preterm populations thought to reflect disturbances of key developmental processes during the neonatal period. The incidence of severe pathology such as periventricular leukomalacia (PVL) has declined (Horbar et al. 2002; Wilson-Costello et al. 2007); however, diffuse white matter changes in the absence of more obvious focal lesions are now the most common abnormality detected by conventional MR imaging. Diffusion tensor imaging (DTI) has revealed diffuse microstructural disturbances in the developing white matter that are dependent on the degree of prematurity at birth and correlated to short-term measures of neurodevelopmental outcome (Huppi et al. 1998; Counsell et al. 2006; Anjari et al. 2007; Krishnan et al. 2007; Ball et al. 2010). In addition, early systemic illness, in the form of chronic lung disease (CLD), has been shown to further exacerbate these alterations and impact negatively on outcome (Short et al. 2003; Anjari et al. 2007; Ball et al. 2010).

Morphometric MR studies have identified cortical disturbances developing before term-equivalent age (Ajayi-Obe et al. 2000; Inder et al. 2005; Kapellou et al. 2006), and widespread cerebral tissue loss is common in the presence of PVL and characterized pathologically by neuronal loss and gliosis (Inder et al. 2005; Pierson et al. 2007; Thompson et al. 2007; Ligam et al. 2009). These observations support the concept of an "encephalopathy of prematurity," a complex of white and gray matter abnormalities that includes disruptions to the thalamocortical system with linked disturbances in the development and function of thalamic nuclei, topographically related cortical regions and connecting white matter tracts (Volpe 2009).

Indeed, even in the absence of severe focal white matter pathology, the subcortical gray matter and, in particular, the thalamus appears specifically vulnerable following preterm birth (Boardman et al. 2006; Srinivasan et al. 2007). Volumetric deficits in the thalamus also appear to be dependent on prematurity at birth and associated with poor functional outcome (Inder et al. 2005; Boardman et al. 2010). Transient developmental processes that underlie thalamocortical connectivity occur during a critical window for vulnerability following preterm birth and disruption of these processes may result in complex cerebral abnormalities (Allendoerfer and Shatz 1994; Volpe 2009; Kostovic and Judas 2010). Here, we examine the thalamocortical system of preterm infants at term-equivalent age, testing the hypothesis that tissue loss in the thalamus is associated with changes in the associated cortical gray matter and macro- and microstructural alterations in the cerebral white matter containing thalamocortical tracts.

Materials and Methods

Ethical permission for this study was granted by the Hammersmith and Queen Charlotte's and Chelsea Hospital (QCCH) Research Ethics Committee. Written parental consent was obtained for each infant.

Subjects

Infants were recruited from the Neonatal Intensive Care Unit at QCCH. All infants born at less than 36 weeks gestational age (as defined by the last menstrual period) between March 2005 and October 2008 who successfully underwent T_1- and T_2-weighted MRI and 15-direction DTI acquisition at term-equivalent age were eligible for inclusion. Infants were excluded if cystic PVL or haemorrhagic parenchymal infarction was apparent on the term-equivalent MRI. Forty-eight infants (67.6%) had evidence of diffuse and excessive high signal intensity (DEHSI) on T_2-weighted scans; 8 infants (11.3%) had evidence of punctuate white matter lesions.

Seventy-four preterm infants (42 male) underwent successful imaging; 3 infants were removed prior to statistical analysis due to unsatisfactory alignment to the reference template. The final cohort of 71 did not differ from the original cohort in gestational age, age at scan, birth weight, or gender. The final cohort (41 male) had a median gestational age of 28 + 5 (range: 23 + 4 to 35 + 2) weeks, a median postmenstrual age at scan of 41 + 5 (38 + 1 to 44 + 4) weeks and median birth weight of 1.11 (0.63–2.87) kg. No infants received postnatal steroids. Across the whole cohort, the median (range) time spent receiving any form of respiratory support was 17 (0–116) days. Fifteen infants had CLD, defined by the need for respiratory support at 36 weeks postmenstrual age. All infants were included in a previously reported study optimizing Tract-Based Spatial Statistics (TBSS) for neonates and examining the effects of prematurity and CLD (Ball et al. 2010).

Imaging

MRI was performed on a Philips 3 T system (Philips Medical Systems, Netherlands) using an 8-channel phased array head coil. T_1-weighted MRI was acquired using: repetition time (TR): 17 ms; echo time (TE): 4.6 ms; flip angle 13°; slice thickness: 1.6 mm; field of view: 210 mm; matrix: 256 × 256 (voxel size: 0.82 × 0.82 × 0.8 mm). T_2-weighted fast-spin echo MRI was acquired using: TR: 8670 ms; TE: 160 ms; flip angle 90°; slice thickness 2 mm; field of view: 220 mm; matrix: 256 × 256 (voxel size: 0.86 × 0.86 × 1 mm). Single-shot echo planar DTI was acquired in 15 noncollinear directions (TR: 8000 ms; TE: 49 ms; slice thickness: 2 mm; field of view: 224 mm; matrix: 128 × 128 (voxel size: 1.75 × 1.75 × 2 mm); b value: 750 s/mm^2; SENSE factor of 2). All examinations were supervised by a pediatrician experienced in MRI procedures. Infants were sedated with oral chloral hydrate (25–50 mg/kg) prior to scanning and pulse oximetry, temperature and electrocardiography data were monitored throughout. Ear protection was used for each infant, comprising earplugs molded from a silicone-based putty (President Putty, Coltene Whaledent, Mahwah, NJ) placed in the external ear and neonatal earmuffs (MiniMuffs, Natus Medical Inc., San Carlos, CA).

Data Analysis

Thalamic Segmentation

The manual placement of regions of interest (ROI) on individual MR images can be subjective and manually intensive and does not easily allow for comparisons across large groups. To avoid this, a single bilateral thalamic mask was manually drawn on the final reference template according to anatomical borders previously described (Srinivasan et al. 2007) (Fig. 1*B*; for details of template construction, see Deformation-Based Morphometry). The high spatial correspondence between each T_1 image and the reference template following nonlinear registration precluded the need to manually place thalamic masks on individual T_1 images. Individual thalamic volume could be estimated by scaling the reference mask volume by the mean Jacobian determinant (a voxelwise measure of volume change between each image and the template, described below) calculated within the mask. To validate, manual thalamic segmentation was performed on T_1 images from 10 randomly selected infants, thalamic volumes measured manually and volumes estimated from the mean Jacobian were consistent (mean difference and limits of agreement = 0.29 ± 1.43; intraclass coefficient = 0.89, $P < 0.001$).

Cortical Segmentation

Cortical segmentation was performed on individual T_2 images using methods specifically optimized for neonatal tissue segmentation (for an example segmentation, see Fig. 1*C*). Images were initially segmented using an expectation–maximization segmentation method driven by age-specific coregistered tissue probability priors obtained from a 4D probabilistic neonatal atlas (Kuklisova-Murgasova et al. 2011). In addition, an automatic 3-step segmentation algorithm was used to remove mislabeled partial volume voxels at the interface of the gray matter and cerebrospinal fluid (Xue et al. 2007).

Deformation-Based Morphometry

Deformation based morphometry (DBM) does not require tissue segmentation or classification and can be used to localize regional variations in tissue volume. The key step is to achieve precise spatial correspondence between each subject's image and a reference template through image registration. The output of each registration is a 3D deformation field representing transformations between each image and the final template. Voxelwise volume change induced by the transformation between each image and the template can be characterized by the determinant of the Jacobian operator applied to the transformation at any given point in the template space, referred to here as the Jacobian. Statistical groupwise analysis of the Jacobian reveals structural volume relative to the group template in an objective voxelwise manner (Ashburner et al. 1998; Rueckert et al. 2003).

After bias correction (FMRIB's Automated Segmentation Tool; FAST v4.1), each MR image was aligned to a chosen target image (gestational age = 28 + 5 weeks; postmenstrual age at scan = 42 + 0 weeks) using linear registration. A reference template was created by taking an intensity average of the aligned images. Each MR image was then aligned to the reference template using a high dimensional registration algorithm based on cubic B-splines (Rueckert et al. 1999, 2003) and averaged to form a second reference template. The nonlinear registration was carried out with successive control point spacing of 20, 10, 5, and 2.5 mm using normalised mutual information information as the similarity metric and the bending energy of the deformation as the smoothness penalty (Gousias et al. 2010). A final set of registrations were performed with the second reference template as the target (Fig. 2). A qualitative evaluation of the alignment accuracy of the transformed images with the template was made before individual deformation fields were used to calculate volume changes. The average intensity template generated from the final set of registrations is shown in Figure 1*A*.

Voxelwise cross-subject statistical analysis of volume relative to the template, represented by the Jacobian, was performed with Randomise (v2.5) as implemented in FMRIB's Software Library (Smith et al. 2004) (FSL v4.1; www.fmrib.ox.ac.uk/fsl). All statistical images were subject to false discovery rate (FDR) correction for multiple comparisons.

Tract-Based Spatial Statistics

DTI analysis was performed using FMRIB's Diffusion Toolbox (FDT v2.0) and Tract-Based Spatial Statistics (Smith et al. 2006) (TBSS v1.2). From each data set, the tensor eigenvalues, λ_1, λ_2, and λ_3, describing the diffusion strength in the primary, secondary, and tertiary diffusion directions, and fractional anisotropy maps were calculated. Individual fractional anisotropy (FA) maps were aligned into a common reference space and a mean FA skeleton, representing the center of all white matter tracts common to the group, was generated using a method optimized for neonatal DTI analysis (Ball et al. 2010). The calculated values of FA, axial diffusivity—the magnitude of λ_1-and radial diffusivity—the mean magnitude of λ_2 and λ_3 were then projected onto this skeleton. Nonparametric permutation-based statistical analysis was performed with Randomise; all diffusion statistics were subject to familywise error (FWE) correction for multiple comparisons following threshold-free cluster enhancement (Smith and Nichols 2009) and are shown at $P < 0.05$.

Statistical Analysis

Further statistical analysis with multiple linear regression was performed with SPSS 17.0 (SPSS Inc., Chicago, IL). In addition to explanatory variables of interest, gestational age at birth, postmenstrual

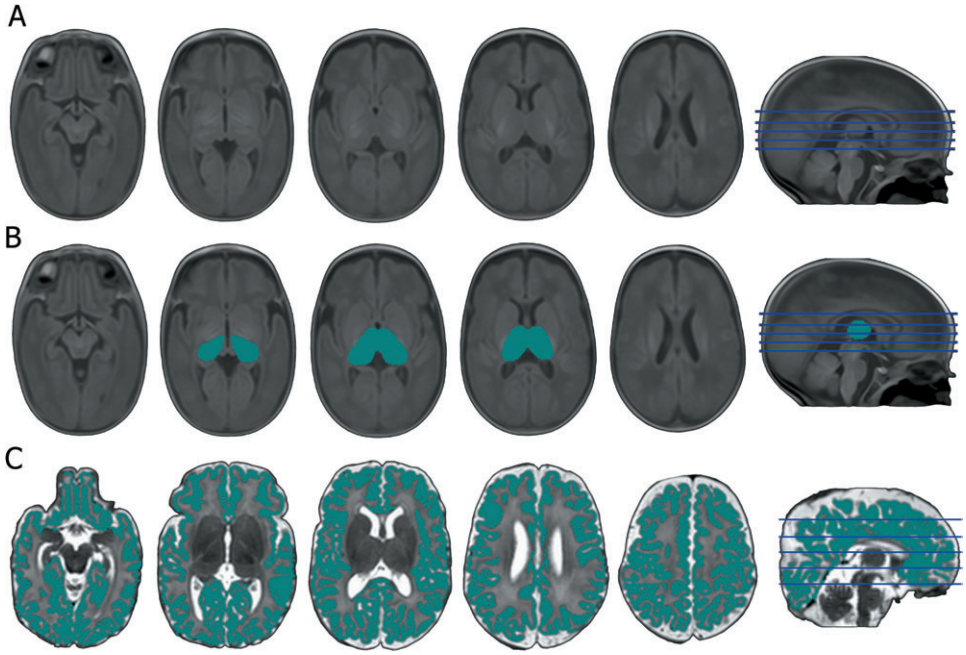

Figure 1. Final reference template and thalamic and cortical segmentations. The final average intensity template is shown in (*A*), the clarity of the subcortical structures and cortical differentiation indicates the accurate alignment of individual images. The mean Jacobian determinant within the mask shown in (*B*) represents the relative volume change between the template and each image and was used to represent thalamic volume across the cohort. A representative example of cortical gray matter segmentation is shown in (*C*).

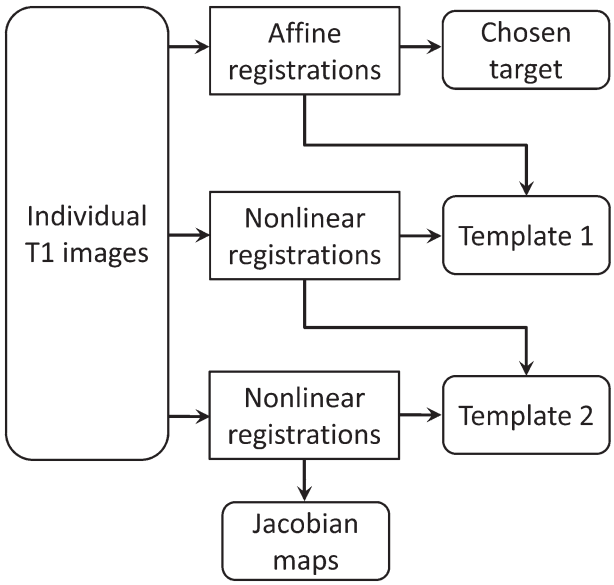

Figure 2. DBM processing pipeline. After preprocessing, T_1 images are affinely aligned to an arbitrarily chosen target MR image and averaged to produce a reference template. Two subsequent iterations of nonlinear registration and template construction produce the final transformations used for analysis.

age at scan, CLD status, and total brain volume were entered into the regression models where stated, partial *r* values are reported.

Results

Regional Brain Volume and Prematurity at Birth

Mean total cortical gray matter volume was 158 (± 26.6) ml. Both cortical gray matter volume and mean thalamic Jacobian (representing thalamic volume) were significantly associated with gestational age at birth, entered into the regression model with the age of each infant at scan (cortical volume: partial $r = 0.37$, $P = 0.002$; thalamic: partial $r = 0.40$, $P = 0.001$; Fig. 3).

DBM was used to locate other brain regions where tissue volume was associated with degree of prematurity at birth. Linear regression revealed significant localized associations between tissue volume (represented voxelwise by the Jacobian) and gestational age at birth (Fig. 4; FDR-corrected for multiple comparisons at $P < 0.01$; minimum *t*-statistic = 2.98). Increasing prematurity was associated with a bilateral pattern of reduced volume present at term-equivalent age and encompassing the anterior temporal lobes, including the hippocampus, the orbitofrontal lobe, and posterior cingulate cortex and extending into the centrum semiovale. Within the deep gray matter, the relationship was most prominent in the thalamus. In addition, discrete clusters were observed in the midbrain and cerebellum. DBM also revealed that increasing prematurity was associated with increasing extra-cerebral CSF, but this did not pass correction for multiple comparisons.

Thalamocortical Development after Preterm Birth

Cortical volume was significantly associated with mean thalamic Jacobian, entered into the regression model with total brain tissue volume (partial $r = 0.32$, $P = 0.007$; Fig. 3*C*). This association remained significant when also including gestational age at birth (partial $r = 0.31$, $P = 0.009$).

After correcting for the effects of prematurity and removing volume change due to individual differences in global brain scaling, DBM revealed significant volumetric covariance between the thalamus and subcortical cerebral tissue (Fig. 5; FDR-corrected $P < 0.001$, minimum *t*-statistic = 3.25). A bilateral pattern was observed comprising white and gray matter proximal to the thalamus and extending into the frontal and temporal lobes, including the hippocampus, through the centrum semiovale into the parietal lobe and, to a lesser

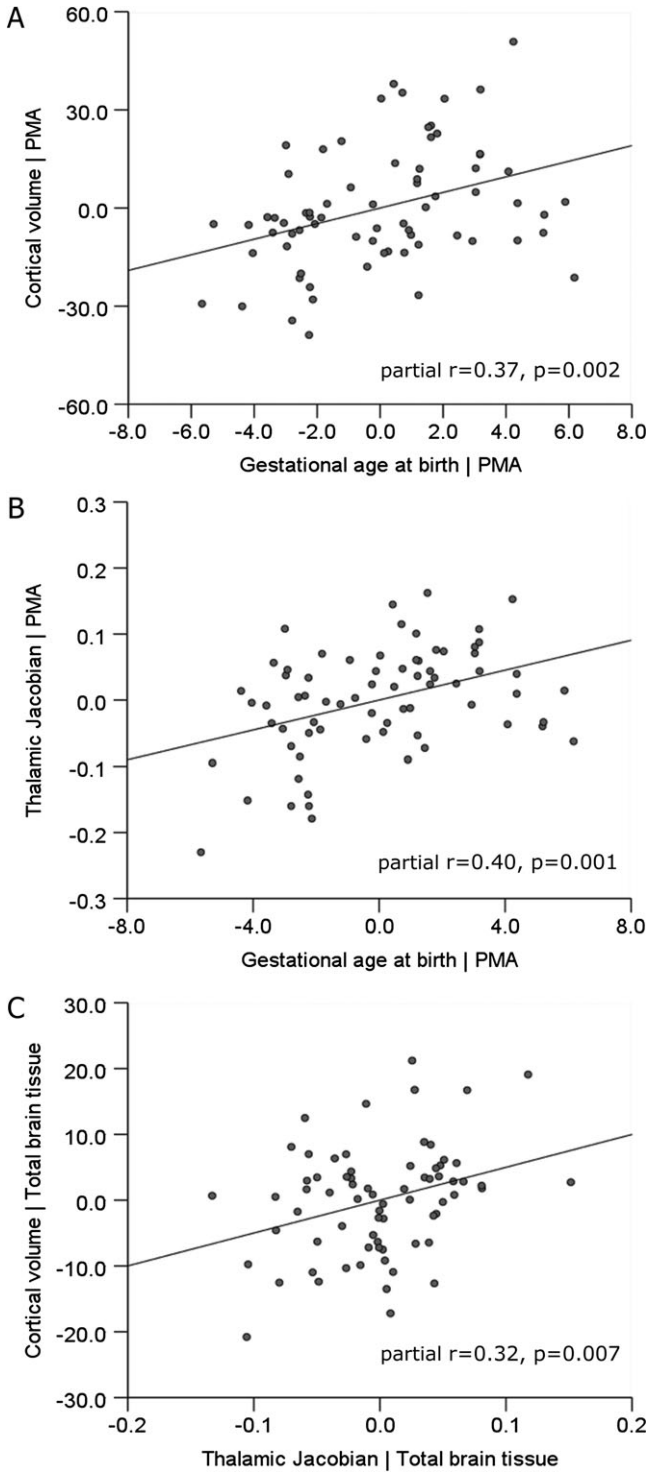

Figure 3. Cortical gray matter volume is correlated with prematurity at birth and thalamic volume at term-equivalent age. Partial regression plots show significant associations between cortical gray matter volume and gestational age at birth (*A*) and mean thalamic Jacobian (representing thalamic volume) and gestational age (*B*), after correction of each measure for the postmenstrual age at scan (PMA) of each infant. Shown in (*C*) is the significant association between cortical volume and thalamic Jacobian, after correction of each for total cerebral tissue volume.

extent, into periventricular white matter in the occipital lobes. This pattern remained highly significant when also covarying for total cortical volume (Supplementary Fig. 1).

In addition to the observed structural associations, TBSS was used to identify where white matter microstructure was associated with thalamic and cortical volume. Increasing thalamic volume at term-equivalent age was significantly associated with FA in the posterior limb of the internal capsule and corpus callosum (including the splenium) after correction for degree of prematurity at birth and the age of each infant when scanned (FWE-corrected for multiple comparison, $P < 0.05$; Fig. 6). Within these regions, linear regression showed that decreasing thalamic volume was independently associated with increasing radial diffusivity (partial $r = -0.34$, $P = 0.004$) but not with axial diffusivity (partial $r = 0.008$) when entered into a model with gestational age at birth and age at scan.

Cortical volume was significantly associated with FA in the posterior corpus callosum after correction for degree of prematurity at birth and age at scan ($P < 0.05$, Fig. 7). In these regions, only radial diffusivity was significantly associated with cortical volume (partial $r = -0.29$, $P = 0.014$; axial diffusivity: partial $r = 0.15$, $P = 0.21$) independent of gestational age and age at scan. Both thalamic and cortical associations remained significant when also correcting for CLD status (Supplementary Fig. 2; CLD defined as requiring respiratory support at 36 weeks postmenstrual age). To investigate the interaction of thalamic and cortical associations with white matter microstructure, a secondary ROI analysis was performed. FA values were extracted from masks in the posterior limb of the internal capsule and posterior corpus callosum (Supplementary Fig. 3). In the internal capsule, FA was significantly associated with thalamic (partial $r = 0.35$, $P = 0.003$) but not cortical volume (partial $r = -0.13$, $P = 0.29$) when both metrics were entered into linear regression alongside gestational age and age at scan (Supplementary Fig. 3*A*). Conversely, FA in the posterior corpus callosum was significantly associated with cortical volume (partial $r = 0.26$, $P = 0.034$) but not with thalamic volume (partial $r = 0.07$, $P = 0.36$; Supplementary Fig. 3*B*).

Finally, to determine how reduced thalamic volume is reflected by the underlying tissue microstructure, mean diffusivity (mean magnitude of λ_1, λ_2, and λ_3) was extracted from each infant's DTI using a thalamic mask transformed onto the DTI reference template. Linear regression revealed that smaller thalamic volume was associated with increased mean thalamic diffusivity when entered into a model with gestational age at birth, total brain volume, and cortical volume (Fig. 8; partial $r = -0.395$, $P = 0.001$). TBSS analysis revealed that thalamic diffusivity was significantly associated with FA in the internal capsule, after correction for degree of prematurity, age at scan, cortical volume, and CLD status (Fig. 8*B*; FWE-corrected $P < 0.05$).

Discussion

These data showed a significant effect of prematurity on thalamic volume related to specific abnormalities in allied brain structures. The effects of prematurity were far-reaching, with reductions in the volume of thalamus, hippocampus, orbitofrontal lobe, posterior cingulate cortex, and centrum semiovale that suggest preterm delivery disrupts specific aspects of cerebral development. However, after this general effect was accounted for, a pattern of structural covariance was observed between the thalamus and particular brain structures, notably in frontotemporal regions, cingulate gyrus, and hippocampus. The observed relation between reduced thalamic and total

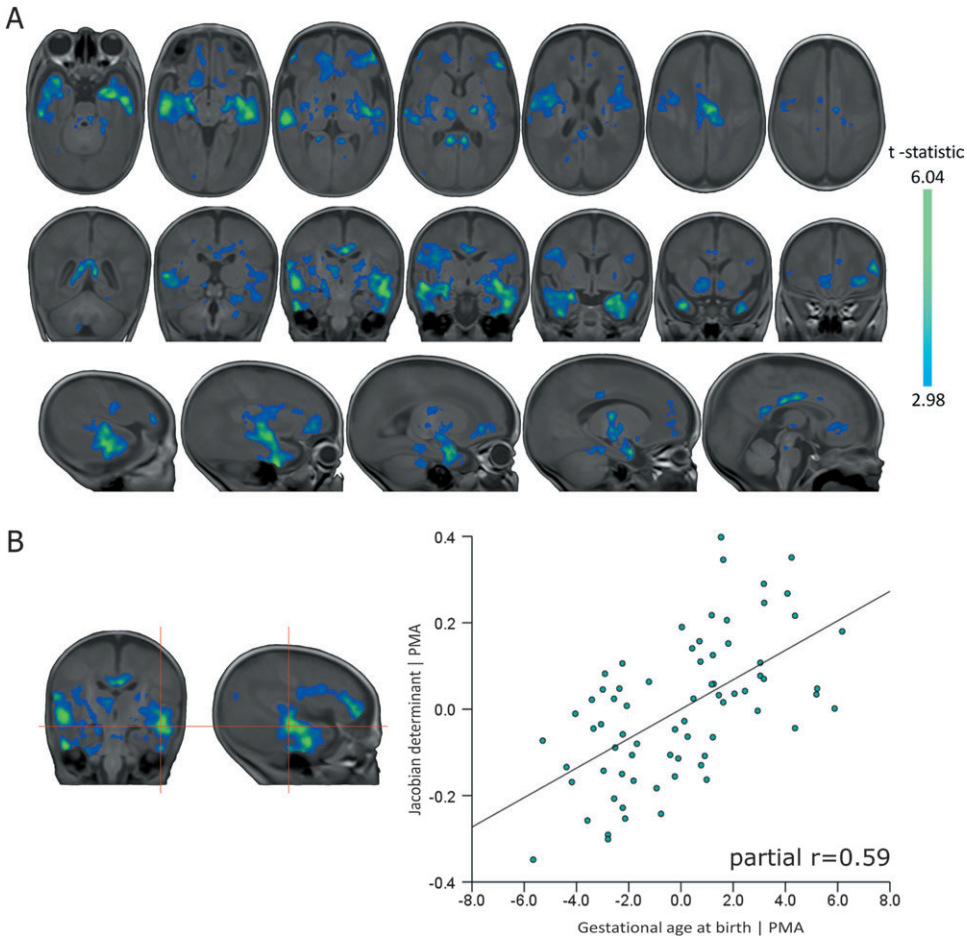

Figure 4. Regional associations between brain tissue volume and prematurity at birth. Regions where tissue volume is significantly associated with gestational age at birth after correcting for the age of each infant at scan are shown in (*A*). Statistical images are corrected for multiple comparisons at $P < 0.01$ FDR-corrected (color bar indicates *t*-statistic). To illustrate this relationship, the Jacobian determinant, representing volume change relative to the reference template, at the site of the maximum *t*-statistic (red crosshairs; $t = 6.04$), was entered into a multiple linear regression with gestational age at birth and age at scan. The partial regression plot (*B*) shows the relationship between Jacobian and gestational age at birth.

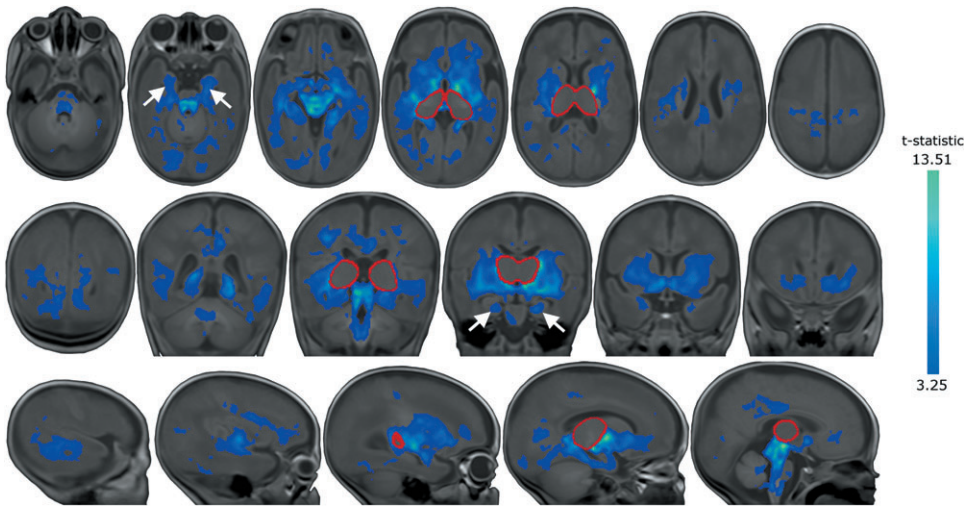

Figure 5. Regional associations between brain tissue volume and thalamic volume at term-equivalent age. Regions where cerebral tissue volume significantly covaried with mean thalamic Jacobian (calculated within the region circled in red). Arrows indicate the hippocampi, statistical images are corrected for multiple comparisons at $P < 0.001$ FDR-corrected (color bar indicates *t*-statistic).

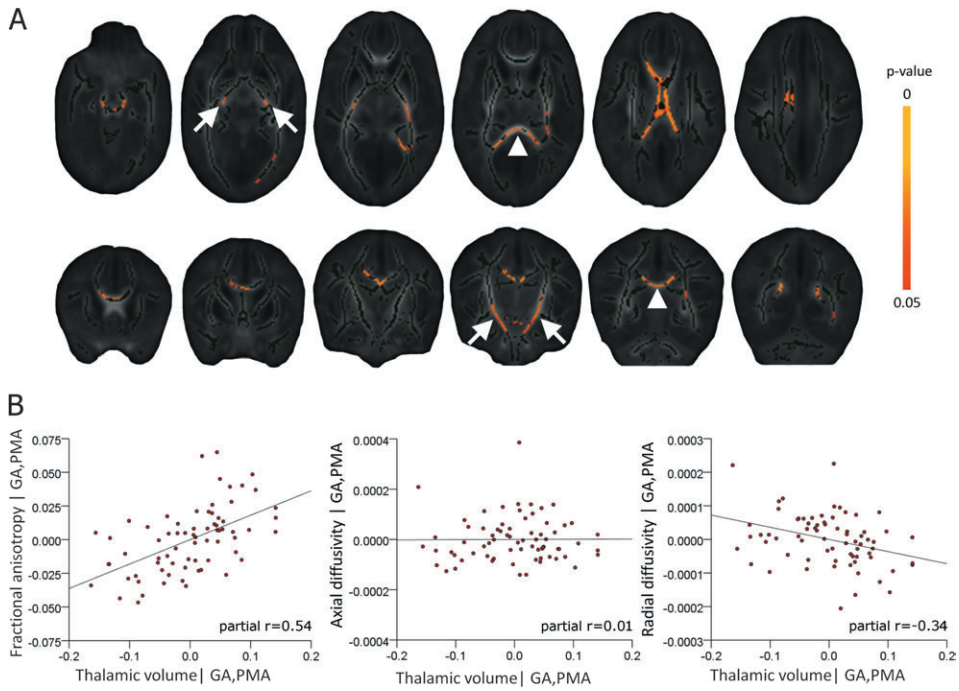

Figure 6. Thalamic volume is associated with white matter microstructure. Regions where fractional anisotropy is significantly associated with thalamic volume, beyond any common association with prematurity at birth and age at imaging, are shown in (*A*). These regions include the posterior limb of the internal capsule (arrows) and the corpus callosum (arrowheads). Images are FWE-corrected at $P < 0.05$ (color bar indicates *P* value), the mean FA skeleton is shown in dark green. Partial regression plots of the relationship between thalamic volume and mean FA, axial diffusivity (AD), and radial diffusivity (RD) extracted from each significant voxel identified in (*A*) and entered into linear regression with gestational age and age at scan are shown in (*B*).

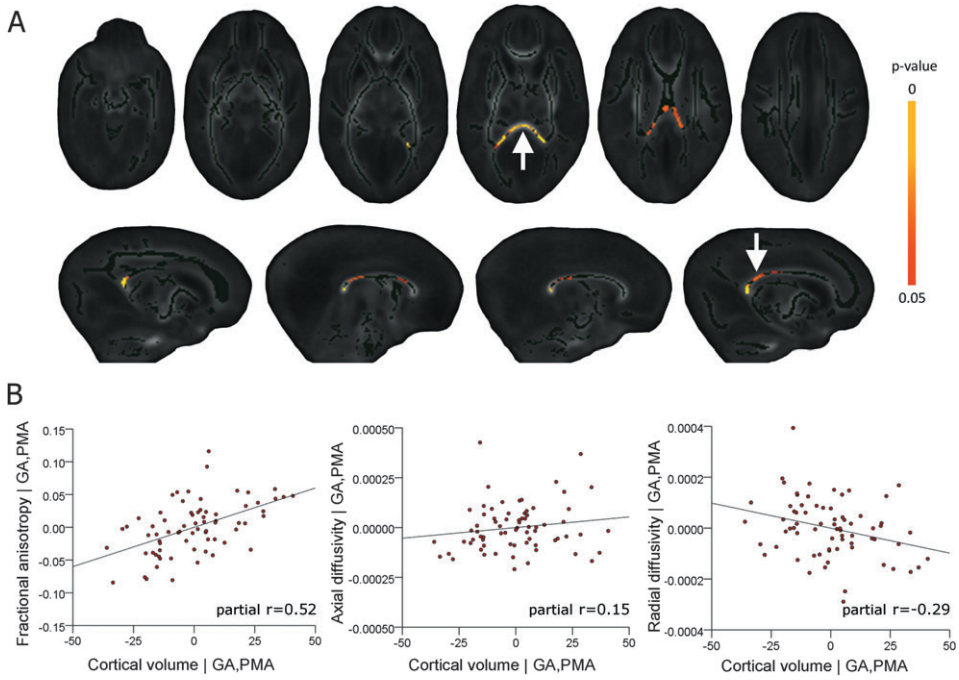

Figure 7. Cortical volume is associated with white matter microstructure. Fractional anisotropy in the posterior corpus callosum (*A*; arrow, bottom row) including the splenium (*A*; arrow, top row) is significantly associated with cortical volume, after correction for prematurity at birth and age at imaging. Images are shown as in Figure 6. Cortical volume and mean FA, AD, and RD extracted from each significant voxel identified in (*A*) were entered into linear regression with gestational age at birth (GA) and age at scan (PMA). Partial regression plots of the relationship between cortical volume and FA, AD and RD, after correction for gestational age and age at scan are shown in (*B*).

cerebral cortical volume together with abnormal thalamic and white matter microstructure suggests the hypothesis that these observations result at least in part from disrupted development of the thalamocortical system.

Previously, altered brain development at term-equivalent age has been detected in preterm infants (Volpe 2009). Studies using tissue segmentation reported that reduced cortical and deep gray matter volumes correlated to neurodevelopmental

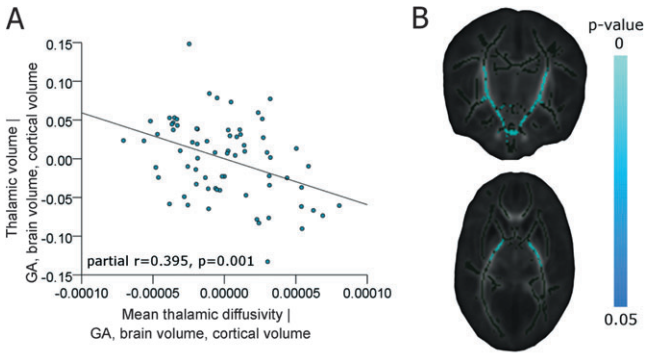

Figure 8. Thalamic diffusivity is associated with thalamic volume and FA in the internal capsule. Thalamic volume (estimated from the mean Jacobian) and mean thalamic diffusivity (estimated from a thalamic mask placed in the DTI reference space) were entered into a multiple linear regression model with gestational age at birth (GA), cortical volume, and total brain volume. The partial regression plot in (*A*) shows the significant association between thalamic volume and thalamic diffusivity. In (*B*), regions where FA was significantly associated with thalamic diffusivity are shown (FWE-corrected at $P < 0.05$), beyond any associations with GA, PMA, cortical volume, and CLD status.

disability at 1 year (Inder et al. 2005) and that reduced cortical surface area predicts neurocognitive abilities at 2 and 6 years (Kapellou et al. 2006; Rathbone et al. 2011). Effects on specific brain structures have been reported, including reduced volume of the hippocampi, although it was not clear if this predicted neurological function independently of white matter pathology (Thompson et al. 2008). Thalamic atrophy and microstructural change have been seen in association with white matter damage (Pierson et al. 2007; Nagasunder et al. 2011), and studies using DBM have shown that the thalamus is specifically vulnerable after preterm birth, particularly in association with white matter pathology (Boardman et al. 2006). Furthermore, a pattern of injury that includes thalamic volume loss and microstructural change in white matter is associated with neurodevelopmental outcome in early childhood (Boardman et al. 2010).

The more detailed pattern of structural covariation reported here shows similarity to the neuroanatomical changes seen in ex-preterm adolescents (Nosarti et al. 2002, 2008; Gimenez et al. 2004; Gimenez, Junque, Narberhaus, et al. 2006; Gimenez, Junque, Vendrell, et al. 2006; Martinussen et al. 2009; Nagy et al. 2009) and is consistent with the development of functional connectivity observed by resting state functional MRI (fMRI) during this period (Fransson et al. 2007; Doria et al. 2010; Smyser et al. 2010). This pattern is also compatible with histological evidence from a primate model of preterm birth and neonatal intensive care that found: decreased white matter volume in the temporal, frontal, and parietal lobes with relative sparing of the occipital lobe and tissue loss in the cortex, deep gray matter, and hippocampi (Dieni et al. 2004; Loeliger et al. 2006, 2009). These results support data suggesting that the neuroanatomical basis for the later sequelae of prematurity develop before the time of normal birth (Rathbone et al. 2011) during the period when the thalamocortical system is forming and essential for normal development (Kostovic and Judas 2010).

The hypothesis that disruption of thalamocortical development underlies the observed changes would suggest an intimate relationship between gray matter structures and connective white matter tracts. We observed that thalamic volume was significantly associated with FA in the internal capsule and the corpus callosum, but subsequent ROI analysis showed that this association only persisted in the internal capsule when cortical volume was also considered. Conversely, cortical volume was only significantly associated with FA in the corpus callosum. Thalamic volume is therefore related to both the microstructure of the thalamic radiations, carrying projection fibers to the cortex, and the volume of the cortex itself. In turn, cortical volume is associated with the microstructure of interhemispheric corticocortical fibers. It is possible that tissue volume in the thalamus and cortex thus reflects thalamocortical connectivity and is dependent on the growth and integrity of connecting white matter tracts.

Reduced thalamocortical volume might also reflect reduced cell and axon numbers in component structures. The number of neurons in topographically connected thalamic and cortical regions is closely related (Stevens 2001) and a large body of histological evidence has determined that both thalamocortical and callosal corticocortical connections are established by term-equivalent age in humans and other primates (Kostovic and Rakic 1984; LaMantia and Rakic 1990; Kostovic and Jovanov-Milosevic 2006). This process can be interrupted by adverse events: cerebral irradiation in mid-to-late pregnancy leads to parallel neuronal loss in the thalamus and cerebral cortex and volume reduction in the subcortical white matter indicating the presence of shared developmental trajectories (Schindler et al. 2002; Selemon et al. 2005, 2009). We found reduced thalamic volume in association with increased mean thalamic diffusivity suggestive of larger extracellular space and compatible with reduced cell density (Beaulieu 2002) and reduced white matter anisotropy with increased radial diffusivity compatible with reduced axon density in associated white matter tracts. Decreased thalamic volume, increased thalamic diffusivity, and increased white matter radial diffusivity are together compatible with decreased cell numbers in the thalamocortical system.

Volpe (2009) argues that brain development in preterm infants is ultimately dependent on a combination of destructive and impaired maturational mechanisms. Here, by removing infants with severe focal lesions such as PVL, we have limited the potential impact of acquired destructive brain lesions on our observations; however, 67% of the cohort had some evidence of DEHSI, thought to reflect diffuse white matter injury possible due to ischemic or hypoxic pathways (Counsell et al. 2003, 2006). Defining normal white matter in the preterm population with conventional MRI is a subjective process; however, by using diffusion metrics such as FA and radial diffusivity (RD), we are able to perform an objective analysis of white matter integrity to capture more fully the spectrum of white matter abnormality present in this population. Additionally, converging evidence suggests that systemic illness in the neonatal period increases the risk of injury and adverse neurodevelopmental outcome (Miller and Ferriero 2009) and we have previously shown in this cohort that CLD is associated with decreased FA and increased RD in the cerebral white matter (Anjari et al. 2009; Ball et al. 2010). Factoring in the presence of CLD status, the pattern of microstructural covariance between the thalamus and the internal capsule and the cortex and corpus callosum remained, although the extent of the associations was reduced. This indicates that numerous injurious processes associated with preterm birth and systemic illness and mediated through inflammatory or excitotoxic

pathways (Arai et al. 1995; Back et al. 2005; Bell et al. 2005; Robinson et al. 2006; Ligam et al. 2009) may potentiate the observed structural and microstructural covariations, possibly with subsequent downstream effects on thalamic volume and development of the overlying cortex (Volpe 2009), resulting in the gestation-dependent pattern of brain development described here. Further investigation during the early neonatal period and longitudinal follow-up of this cohort may help elucidate the nature and evolution of maldevelopment in white matter, deep gray matter, and cerebrum as a whole in this population.

It should be noted that the DBM analyses did not reveal significant associations in the cortex. This was not unexpected: DBM is highly sensitive to local volume change that is spatially consistent across the whole group and thus relies on precise spatial correspondence without reliance on tissue classification and spatial smoothing, however due to the rapid increases in cortical complexity during the neonatal period (Kapellou et al. 2006) and limitations in current image registration techniques for neonates, achieving precise correspondence in cortical regions remains difficult. By combining DBM with cortical segmentations in native image space, we were still able to capture information from the whole brain in this cohort.

In summary, we have shown that at term-equivalent age and in the absence of severe white matter injury, preterm infants show a detailed pattern of altered brain structure and microstructure that mirror changes seen in adolescent ex-preterm infants and are compatible with disruption of thalamocortical development.

Supplementary Material

Supplementary material can be found at: http://www.cercor.oxfordjournals.org/

Notes

We are grateful for support from the Imperial College Healthcare Comprehensive Biomedical Research Centre Funding Scheme, the Medical Research Council (UK), the Academy of Medical Sciences, The Health Foundation and Philips Medical Systems for research grant support. We thank the families who took part in the study and our colleagues in the Neonatal Intensive Care Unit at QCCH. *Conflict of Interest* : None declared.

References

Ajayi-Obe M, Saeed N, Cowan FM, Rutherford MA, Edwards AD. 2000. Reduced development of cerebral cortex in extremely preterm infants. Lancet. 356:1162–1163.

Allendoerfer KL, Shatz CJ. 1994. The subplate, a transient neocortical structure: its role in the development of connections between thalamus and cortex. Annu Rev Neurosci. 17:185–218.

Anjari M, Counsell SJ, Srinivasan L, Allsop JM, Hajnal JV, Rutherford MA, Edwards AD. 2009. The association of lung disease with cerebral white matter abnormalities in preterm infants. Pediatrics. 124:268–276.

Anjari M, Srinivasan L, Allsop JM, Hajnal JV, Rutherford MA, Edwards AD, Counsell SJ. 2007. Diffusion tensor imaging with tract-based spatial statistics reveals local white matter abnormalities in preterm infants. Neuroimage. 35:1021–1027.

Arai Y, Deguchi K, Mizuguchi M, Takashima S. 1995. Expression of beta-amyloid precursor protein in axons of periventricular leukomalacia brains. Pediatr Neurol. 13:161–163.

Ashburner J, Hutton C, Frackowiak R, Johnsrude I, Price C, Friston K. 1998. Identifying global anatomical differences: deformation-based morphometry. Hum Brain Mapp. 6:348–357.

Back SA, Luo NL, Mallinson RA, O'Malley JP, Wallen LD, Frei B, Morrow JD, Petito CK, Roberts CT, Jr, Murdoch GH, et al. 2005. Selective vulnerability of preterm white matter to oxidative damage defined by F2-isoprostanes. Ann Neurol. 58:108–120.

Ball G, Counsell SJ, Anjari M, Merchant N, Arichi T, Doria V, Rutherford MA, Edwards AD, Rueckert D, Boardman JP. 2010. An optimised tract-based spatial statistics protocol for neonates: applications to prematurity and chronic lung disease. Neuroimage. 53:94–102.

Beaulieu C. 2002. The basis of anisotropic water diffusion in the nervous system—a technical review. NMR Biomed. 15:435–455.

Bell JE, Becher JC, Wyatt B, Keeling JW, McIntosh N. 2005. Brain damage and axonal injury in a Scottish cohort of neonatal deaths. Brain. 128:1070–1081.

Boardman JP, Counsell SJ, Rueckert D, Kapellou O, Bhatia KK, Aljabar P, Hajnal J, Allsop JM, Rutherford MA, Edwards AD. 2006. Abnormal deep grey matter development following preterm birth detected using deformation-based morphometry. Neuroimage. 32:70–78.

Boardman JP, Craven C, Valappil S, Counsell SJ, Dyet LE, Rueckert D, Aljabar P, Rutherford MA, Chew AT, Allsop JM, et al. 2010. A common neonatal image phenotype predicts adverse neurodevelopmental outcome in children born preterm. Neuroimage. 52:409–414.

Counsell SJ, Allsop JM, Harrison MC, Larkman DJ, Kennea NL, Kapellou O, Cowan FM, Hajnal JV, Edwards AD, Rutherford MA. 2003. Diffusion-weighted imaging of the brain in preterm infants with focal and diffuse white matter abnormality. Pediatrics. 112:1–7.

Counsell SJ, Shen Y, Boardman JP, Larkman DJ, Kapellou O, Ward P, Allsop JM, Cowan FM, Hajnal JV, Edwards AD, et al. 2006. Axial and radial diffusivity in preterm infants who have diffuse white matter changes on magnetic resonance imaging at term-equivalent age. Pediatrics. 117:376–386.

Delobel-Ayoub M, Arnaud C, White-Koning M, Casper C, Pierrat V, Garel M, Burguet A, Roze JC, Matis J, Picaud JC, et al. 2009. Behavioral problems and cognitive performance at 5 years of age after very preterm birth: the EPIPAGE study. Pediatrics. 123:1485–1492.

Dieni S, Inder T, Yoder B, Briscoe T, Camm E, Egan G, Denton D, Rees S. 2004. The pattern of cerebral injury in a primate model of preterm birth and neonatal intensive care. J Neuropathol Exp Neurol. 63:1297–1309.

Doria V, Beckmann CF, Arichi T, Merchant N, Groppo M, Turkheimer FE, Counsell SJ, Murgasova M, Aljabar P, Nunes RG, et al. 2010. Emergence of resting state networks in the preterm human brain. Proc Natl Acad Sci U S A. 107:20015–20020.

Fransson P, Skiold B, Horsch S, Nordell A, Blennow M, Lagercrantz H, Aden U. 2007. Resting-state networks in the infant brain. Proc Natl Acad Sci U S A. 104:15531–15536.

Gimenez M, Junque C, Narberhaus A, Botet F, Bargallo N, Mercader JM. 2006. Correlations of thalamic reductions with verbal fluency impairment in those born prematurely. Neuroreport. 17:463–466.

Gimenez M, Junque C, Narberhaus A, Caldu X, Salgado-Pineda P, Bargallo N, Segarra D, Botet F. 2004. Hippocampal gray matter reduction associates with memory deficits in adolescents with history of prematurity. Neuroimage. 23:869–877.

Gimenez M, Junque C, Vendrell P, Narberhaus A, Bargallo N, Botet F, Mercader JM. 2006. Abnormal orbitofrontal development due to prematurity. Neurology. 67:1818–1822.

Gousias IS, Hammers A, Heckemann RA, Counsell SJ, Dyet LE, Boardman JP, Edwards AD, Rueckert D. 2010. Atlas selection strategy for automatic segmentation of pediatric brain MRIs into 83 ROIs. In: Imaging Systems and Techniques (IST), 2010 IEEE International Conference on. p. 290–293 doi: 10.1109/IST.2010.5548493.

Horbar JD, Badger GJ, Carpenter JH, Fanaroff AA, Kilpatrick S, LaCorte M, Phibbs R, Soll RF. Members of the Vermont Oxford Network. 2002. Trends in mortality and morbidity for very low birth weight infants, 1991–1999. Pediatrics. 110:143–151.

Huppi PS, Maier SE, Peled S, Zientara GP, Barnes PD, Jolesz FA, Volpe JJ. 1998. Microstructural development of human newborn cerebral white matter assessed in vivo by diffusion tensor magnetic resonance imaging. Pediatr Res. 44:584–590.

Inder TE, Warfield SK, Wang H, Huppi PS, Volpe JJ. 2005. Abnormal cerebral structure is present at term in premature infants. Pediatrics. 115:286–294.

Kapellou O, Counsell SJ, Kennea N, Dyet L, Saeed N, Stark J, Maalouf E, Duggan P, Ajayi-Obe M, Hajnal J, et al. 2006. Abnormal cortical development after premature birth shown by altered allometric scaling of brain growth. PLoS Med. 3:e265.

Kostovic I, Jovanov-Milosevic N. 2006. The development of cerebral connections during the first 20–45 weeks' gestation. Semin Fetal Neonatal Med. 11:415–422.

Kostovic I, Judas M. 2010. The development of the subplate and thalamocortical connections in the human foetal brain. Acta Paediatr. 99:1119–1127.

Kostovic I, Rakic P. 1984. Development of prestriate visual projections in the monkey and human fetal cerebrum revealed by transient cholinesterase staining. J Neurosci. 4:25–42.

Krishnan ML, Dyet LE, Boardman JP, Kapellou O, Allsop JM, Cowan F, Edwards AD, Rutherford MA, Counsell SJ. 2007. Relationship between white matter apparent diffusion coefficients in preterm infants at term-equivalent age and developmental outcome at 2 years. Pediatrics. 120:e604–e609.

Kuklisova-Murgasova M, Aljabar P, Srinivasan L, Counsell SJ, Doria V, Serag A, Gousias IS, Boardman JP, Rutherford MA, Edwards AD, et al. 2011. A dynamic 4D probabilistic atlas of the developing brain. Neuroimage. 54:2750–2763.

LaMantia AS, Rakic P. 1990. Axon overproduction and elimination in the corpus callosum of the developing rhesus monkey. J Neurosci. 10:2156–2175.

Ligam P, Haynes RL, Folkerth RD, Liu L, Yang M, Volpe JJ, Kinney HC. 2009. Thalamic damage in periventricular leukomalacia: novel pathologic observations relevant to cognitive deficits in survivors of prematurity. Pediatr Res. 65:524–529.

Loeliger M, Inder T, Cain S, Ramesh RC, Camm E, Thomson MA, Coalson J, Rees SM. 2006. Cerebral outcomes in a preterm baboon model of early versus delayed nasal continuous positive airway pressure. Pediatrics. 118:1640–1653.

Loeliger M, Inder TE, Shields A, Dalitz P, Cain S, Yoder B, Rees SM. 2009. High-frequency oscillatory ventilation is not associated with increased risk of neuropathology compared with positive pressure ventilation: a preterm primate model. Pediatr Res. 66:545–550.

Marlow N, Wolke D, Bracewell MA, Samara M. EPICure Study Group. 2005. Neurologic and developmental disability at six years of age after extremely preterm birth. N Engl J Med. 352:9–19.

Martinussen M, Flanders DW, Fischl B, Busa E, Lohaugen GC, Skranes J, Vangberg TR, Brubakk AM, Haraldseth O, Dale AM. 2009. Segmental brain volumes and cognitive and perceptual correlates in 15-year-old adolescents with low birth weight. J Pediatr. 155:848–853.e1.

Miller SP, Ferriero DM. 2009. From selective vulnerability to connectivity: insights from newborn brain imaging. Trends Neurosci. 32:496–505.

Nagasunder AC, Kinney HC, Bluml S, Tavare CJ, Rosser T, Gilles FH, Nelson MD, Panigrahy A. 2011. Abnormal microstructure of the atrophic thalamus in preterm survivors with periventricular leukomalacia. AJNR Am J Neuroradiol. 32:185–191.

Nagy Z, Ashburner J, Andersson J, Jbabdi S, Draganski B, Skare S, Bohm B, Smedler AC, Forssberg H, Lagercrantz H. 2009. Structural correlates of preterm birth in the adolescent brain. Pediatrics. 124:e964–e972.

Nosarti C, Al-Asady MH, Frangou S, Stewart AL, Rifkin L, Murray RM. 2002. Adolescents who were born very preterm have decreased brain volumes. Brain. 125:1616–1623.

Nosarti C, Giouroukou E, Healy E, Rifkin L, Walshe M, Reichenberg A, Chitnis X, Williams SC, Murray RM. 2008. Grey and white matter distribution in very preterm adolescents mediates neurodevelopmental outcome. Brain. 131:205–217.

Pierson CR, Folkerth RD, Billiards SS, Trachtenberg FL, Drinkwater ME, Volpe JJ, Kinney HC. 2007. Gray matter injury associated with periventricular leukomalacia in the premature infant. Acta Neuropathol. 114:619–631.

Rathbone R, Counsell SJ, Kapellou O, Dyet L, Kennea N, Hajnal JV, Allsop JM, Cowan FM, Edwards AD. Forthcoming 2011. Perinatal cortical growth and childhood neurocognitive abilities. Neurology.

Robinson S, Li Q, Dechant A, Cohen ML. 2006. Neonatal loss of gamma-aminobutyric acid pathway expression after human perinatal brain injury. J Neurosurg. 104:396–408.

Rueckert D, Frangi AF, Schnabel JA. 2003. Automatic construction of 3-D statistical deformation models of the brain using nonrigid registration. IEEE Trans Med Imaging. 22:1014–1025.

Rueckert D, Sonoda LI, Hayes C, Hill DL, Leach MO, Hawkes DJ. 1999. Nonrigid registration using free-form deformations: application to breast MR images. IEEE Trans Med Imaging. 18:712–721.

Schindler MK, Wang L, Selemon LD, Goldman-Rakic PS, Rakic P, Csernansky JG. 2002. Abnormalities of thalamic volume and shape detected in fetally irradiated rhesus monkeys with high dimensional brain mapping. Biol Psychiatry. 51:827–837.

Selemon LD, Begovic A, Rakic P. 2009. Selective reduction of neuron number and volume of the mediodorsal nucleus of the thalamus in macaques following irradiation at early gestational ages. J Comp Neurol. 515:454–464.

Selemon LD, Wang L, Nebel MB, Csernansky JG, Goldman-Rakic PS, Rakic P. 2005. Direct and indirect effects of fetal irradiation on cortical gray and white matter volume in the macaque. Biol Psychiatry. 57:83–90.

Short EJ, Klein NK, Lewis BA, Fulton S, Eisengart S, Kercsmar C, Baley J, Singer LT. 2003. Cognitive and academic consequences of bronchopulmonary dysplasia and very low birth weight: 8-year-old outcomes. Pediatrics. 112:e359.

Smith SM, Jenkinson M, Johansen-Berg H, Rueckert D, Nichols TE, Mackay CE, Watkins KE, Ciccarelli O, Cader MZ, Matthews PM, et al. 2006. Tract-based spatial statistics: voxelwise analysis of multi-subject diffusion data. Neuroimage. 31:1487–1505.

Smith SM, Jenkinson M, Woolrich MW, Beckmann CF, Behrens TE, Johansen-Berg H, Bannister PR, De Luca M, Drobnjak I, Flitney DE, et al. 2004. Advances in functional and structural MR image analysis and implementation as FSL. Neuroimage. 23(Suppl 1): S208–S219.

Smith SM, Nichols TE. 2009. Threshold-free cluster enhancement: addressing problems of smoothing, threshold dependence and localisation in cluster inference. Neuroimage. 44:83–98.

Smyser CD, Inder TE, Shimony JS, Hill JE, Degnan AJ, Snyder AZ, Neil JJ. 2010. Longitudinal analysis of neural network development in preterm infants. Cereb Cortex. 20:2852–2862.

Srinivasan L, Dutta R, Counsell SJ, Allsop JM, Boardman JP, Rutherford MA, Edwards AD. 2007. Quantification of deep gray matter in preterm infants at term-equivalent age using manual volumetry of 3-Tesla magnetic resonance images. Pediatrics. 119:759–765.

Stevens CF. 2001. An evolutionary scaling law for the primate visual system and its basis in cortical function. Nature. 411:193–195.

Thompson DK, Warfield SK, Carlin JB, Pavlovic M, Wang HX, Bear M, Kean MJ, Doyle LW, Egan GF, Inder TE. 2007. Perinatal risk factors altering regional brain structure in the preterm infant. Brain. 130:667–677.

Thompson DK, Wood SJ, Doyle LW, Warfield SK, Lodygensky GA, Anderson PJ, Egan GF, Inder TE. 2008. Neonate hippocampal volumes: prematurity, perinatal predictors, and 2-year outcome. Ann Neurol. 63:642–651.

Volpe JJ. 2009. Brain injury in premature infants: a complex amalgam of destructive and developmental disturbances. Lancet Neurol. 8:110–124.

Wilson-Costello D, Friedman H, Minich N, Siner B, Taylor G, Schluchter M, Hack M. 2007. Improved neurodevelopmental outcomes for extremely low birth weight infants in 2000–2002. Pediatrics. 119:37–45.

Xue H, Srinivasan L, Jiang S, Rutherford M, Edwards AD, Rueckert D, Hajnal JV. 2007. Automatic segmentation and reconstruction of the cortex from neonatal MRI. Neuroimage. 38:461–477.